Sensitivity Analysis and Uncertainty Quantification in PWR Irradiation Ageing like problems

Juan A. Monleón de la Lluvia[1], Mariya Brovchenko[1], Dimitri Rochman[2], Eric Dumonteil[3]

[1]Institut de Radioprotection et de Sûreté Nucléaire (IRSN), PSN-RES/SNC/LN, Fontenay-aux-Roses 92260, France
[2]Paul Scherrer Institute (PSI), Villigen 5232, Switzerland
[3]Université Paris-Saclay, CEA, Institut de Recherche sur les Lois Fondamentales de l'Univers, 91191, Gif-sur-Yvette, France
juan-antonio.monleondelalluvia@irsn.fr

[Placeholder for Digital Object Identifier (DOI) to be added by ANS]

INTRODUCTION

The lifespan of nuclear power plants is a critical aspect of energy production, with reactor vessel ageing being one of the main challenges. Over time, ageing under neutron irradiation of the Pressurized Water Reactor (PWR) vessels leads to changes in the material's micro-structure. These changes adversely affect the mechanical properties, making the material more brittle and susceptible to fractures, especially under strong temperature gradients. Beyond the vessel, the aging of other elements, such as concrete structures, also poses significant concerns. Accurate calculations of neutron fluence and the associated uncertainties throughout and beyond the reactor vessel are essential to ensure safety. This study aims at addressing this issue by applying a specific methodology to a simplified model, providing a foundational step to quantify the uncertainty in Monte-Carlo simulations related to irradiation ageing in nuclear reactors.

Propagation of uncertainties in neutron transport calculations determines how uncertainties in various input quantities, such as nuclear data, affect responses like k_{eff} in criticality problems, and flux or reaction rates in both criticality and fixed source problems. For propagating nuclear data uncertainties, there are two main methods used: Total Monte Carlo (TMC), based on random sampling of the nuclear data, and the Perturbation Method [1]. In this work, the focus on the latter method is given. This method relies on the calculation of sensitivity coefficients as a way of quantifying the effect that small perturbations in input parameters have on certain output responses. Its advantage lies in computational efficiency and quick insights into the influence of specific parameters on results.

The Perturbation Method uses the Sandwich Formula [2] to propagate nuclear data uncertainties:

$$\sigma^{ND} = \sqrt{S \cdot Cov \cdot S^T} \qquad (1)$$

where S and S^T are the sensitivity vector and its transpose, and Cov is the nuclear data variance-covariance matrix. Thus, this is a first-order approximation for the uncertainty propagation. To perform this type of uncertainty propagation, it is necessary to first obtain the sensitivity coefficients that constitute the sensitivity vector. Different Monte Carlo codes have different ways of implementing the calculation of sensitivity coefficients. For fixed source problems, there are three main methods: Generalized Perturbation Theory (GPT) [3], Differential Operator Sampling (DOS) [4], and Correlated Sampling (CS) [5].

In this study, we focus on the fixed source problem, as used for the neutron transport from the core through the vessel and the methodology to obtain the sensitivity coefficients with a Monte Carlo code using a simple model. The robustness of the obtained values is verified using different methods (GPT and DOS), and the effect of the use of variance reduction methods is quantified. Additionally, we checked the limits of the first-order sensitivity approach by comparing it to second-order perturbed response and direct perturbation. Finally, the main contributors to the final nuclear data uncertainties are provided.

METHODOLOGY

There is increasing interest in using SERPENT's GPT collision history-based implementation [6,7] for shielding problems due to its versatility and ease of use, though some works have noted limitations in memory consumption [8]. MCNP uses a DOS implementation via PERT cards, which estimate Taylor series coefficients up to the second order. These coefficients are used to calculate responses for any perturbed value [4], which can be used to obtain the sensitivity coefficients. However, focusing on the complexity of the implementation of each method, SERPENT's approach is considerably simpler to use. It is possible to obtain sensitivity coefficients directly for different isotopes, reactions, and energies in just one simulation, while PERT cards require the definition of at least two cards for each isotope, reaction, and energy bin. For example, if one were to consider four reactions for five different isotopes in a 44 energy-grid structure, it would need defining 2x4x5x44=1760 cards. Additionally, the output from PERT cards are Taylor series coefficients, which require further post-processing to obtain the sensitivity coefficients. New features like the FSENS card are being developed [9] to calculate fixed source sensitivities in a much more user-friendly way with promising results, but they are not yet available in MCNP6.3 and not accessible to the authors.

For our study, we obtained the sensitivity coefficients using SERPENT2.2 (GPT) and MCNP6.3 (DOS) in a simple spherical geometry with concentric layers of air, water, and steel (see Table I). This model aims at illustrating the neutron travel path from the core through the vessel in a PWR. The materials used include borated water with 10 ppm of Boron, air composed of 14N and 16O, and 16MND5 steel. The complete inputs for replication of results are available for free access at GitLab[a].

Table I. Layer Specifications of Spherical Geometry

Material	Inner Radius (cm)	Thickness (cm)
Air	0	162
Steel	162	3
Water	165	5
Steel	170	5
Water	175	6.15
Steel	181.15	6.5
Water	187.65	11.75
Steel	199.4	20
Air/Detector	219.4	1
Air	220.4	79.6

The neutron source was a point source emitting neutrons in the energy range of 1-3 MeV, with no emission outside this range. The detector, positioned after the last steel spherical shell, was a concentric spherical shell 1 cm thick. Neutron flux was scored in this detector and divided into three responses according to energy ranges: [0-0.1], [0.1-1.0], and [1.0-3.0] MeV. For transport calculations, we used the ENDF/B-VIII.0 nuclear data library with the same ACE files in both transport codes. Sensitivity coefficients were calculated using the SCALE 6.1 44-group energy grid [11]. The variance-covariance matrix from the same set was then used in the Sandwich Formula to propagate nuclear data uncertainties. This matrix is built from various ENDFB evaluations and JENDL-3.3, as detailed in [11]. Focusing on the methodology, the consistency of the nuclear data libraries is not of the main interest to the authors in this study.

The sensitivity coefficients and the nuclear data uncertainty propagation were performed considering all isotopes present in water: 1H (11.19%), 16O (88.83%), 10B (0.00018%), and 11B (0.00082%), and the following nuclides from the steel: 12C (0.20%), 28Si (0.18%), 52Cr (0.21%), 55Mn (1.35%), 54Fe (5.42%), 56Fe (88.88%), 57Fe (2.12%), 58Fe (0.29%), 58Ni (0.44%), 60Ni (0.17%), and 100Mo (0.05%), that sums up to 99.31%, all given in weight percent (wt%). The cross sections were perturbed simultaneously in all cells where the nuclide was present.

Variance reduction methods for the sensitivity calculations were carried out in MCNP using ADVANTG3.2 [12] for the generation of the weight windows parameters. The CADIS method, which uses deterministic calculation of the adjoint flux, was applied with SCALE-6.1 27n19g library. ADVANTG generated weight windows using the same energy grid on a rectangular 3D mesh with dimensions of 162x162x162 voxels. Thus, the detector was spanned over a large number of cells and its energy integrated neutron flux was used as a single response in the ADVANTG calculation. Additionally, we applied weight windows directly on the geometry cells in MCNP using the WWN card. The weight window parameters were defined by the authors "manually" with a regular division by 2 in each steel or water filled cell. This approach is expected to be less optimal but allows the weight windows to better match the problem's geometry.

To verify the robustness of the calculations, direct perturbations were applied to the total cross sections by altering the density. The sensitivity coefficients were then calculated using the central difference method from two independent simulations as:

$$S_x^R = \frac{(R_p - R_n)}{2 \cdot \mathrm{R}_0 \cdot \Delta x/x} \quad (2)$$

where S_x^R is the relative sensitivity coefficient, R_p and R_n are the responses to positive and negative perturbations, R_0 the unperturbed response and $\Delta x/x$ the relative perturbation. Equation (2) was used to calculate the sensitivity coefficient for direct perturbations in both codes and for the DOS method results in MCNP. It was not applied for the GPT method in SERPENT, as SERPENT provides the sensitivity coefficients directly.

RESULTS

Sensitivity Analysis

MCNP sensitivities do not show a response to total inelastic reactions (MT=4). Instead, inelastic reactions were compared using MT=51 and MT=52, which correspond to inelastic scattering with residuals in the 1st and 2nd energy states, respectively.

Figure 1 shows the comparison of sensitivity profiles for Fe56 between four sets of results: SERPENT, MCNP-analog (without weight windows), MCNP-ADV (with weight windows generated by ADVANTG), and MCNP-WWN (with weight windows linked to the geometrical cells via the WWN card). The plots display these profiles along with 1 standard deviation of the statistical uncertainties. For the calculation of uncertainties, the covariance between terms when using MCNP PERT cards was proven to be negligible and thus was not considered.

Focusing first on the behavior between SERPENT and analog MCNP, we observe a good agreement for all nuclides and reactions studied. However, an important observation needs to be noted: SERPENT appears to have a threshold effect when calculating small sensitivities. For instance, it yields 0 sensitivity for proton (MT=103) and alpha

production (MT=107) reactions, while MCNP shows very small but non-zero sensitivity values.

Regarding sensitivities obtained with weight windows generated by ADVANTG, a clear bias is observed in the profiles. In nuclides where both elastic and inelastic reactions occur, such as 56Fe, the elastic reaction is underestimated while the rest of the reactions, particularly inelastic, are overestimated (see Figure 1). These effects compensate each other and produce a sensitivity profile for the total cross section very close to the one given by the analog simulation. On the other hand, in nuclides where little to no inelastic reactions occur and where elastic scattering dominates, such as H1 (see Figure 2), no clear bias is observed. Additionally,

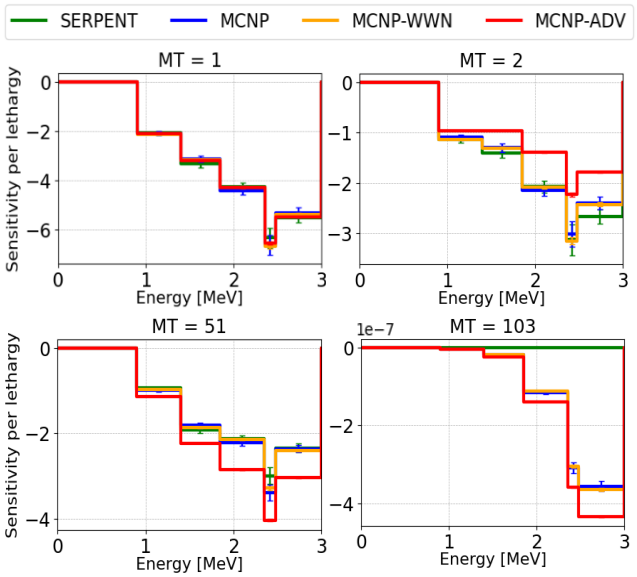

Fig. 1. Sensitivity profiles for 56Fe for different reactions: total (MT=1), elastic (MT=2), inelastic (MT=51), and proton production (MT=103). The x-axis shows the energy range where perturbations were applied. The sensitivity profiles show the effect of perturbations on the detector response for neutrons in the 1-3 MeV range.

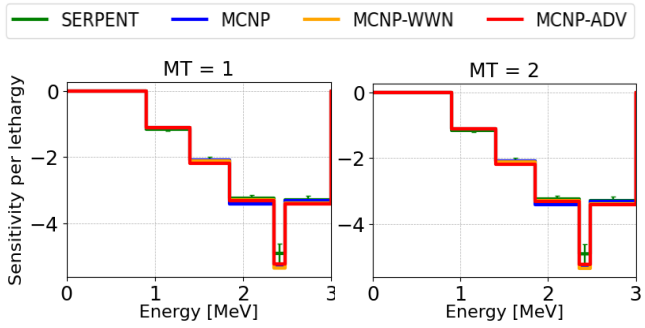

Fig. 2. Sensitivity profiles for 1H for total (MT=1) and elastic (MT=2) reactions. The x-axis shows the energy range where perturbations were applied. The sensitivity profiles show the effect of perturbations on the detector response for neutrons in the 1-3 MeV range.

the results from MCNP-WWN do not introduce any significant bias on sensitivities and the agreement with both SERPENT and MCNP-Analog is very good.

Comparing simulation convergence and efficiency between MCNP analog and variance-reduced simulations, we observe a clear improvement in the main indicators: error, variance of variance, slope, and FOM. Table II presents result for a specific case as an example.

Table II. Statistical checks for the first-order Taylor coefficient using the PERT card in MCNP for the Fe56 elastic cross section reaction from 2.479 to 3.0 MeV.

Simulation	Error	VOV	Slope	FOM
Analog	0.0219	0.0014	4.7	1.6
WWN	0.0067	0.0001	7.4	7.9
ADVANTG	0.0060	0.0000*	10.0	17

*Corresponding to <0.0001 due to digit number limitation.

Continuing the analysis, integral total cross section sensitivities for 56Fe were calculated and compared using the different methodologies. Perturbations were studied for 1%, 2%, 3%, 4%, 5% and 10% with 5% results shown in Figure 3 with three standard deviations of statistical uncertainties.

All sensitivity coefficients, regardless of the method used, show consistent results. The neutron flux sensitivity is notably higher in the 1-3 MeV energy range, where it is approximately twice as large compared to lower energy ranges.

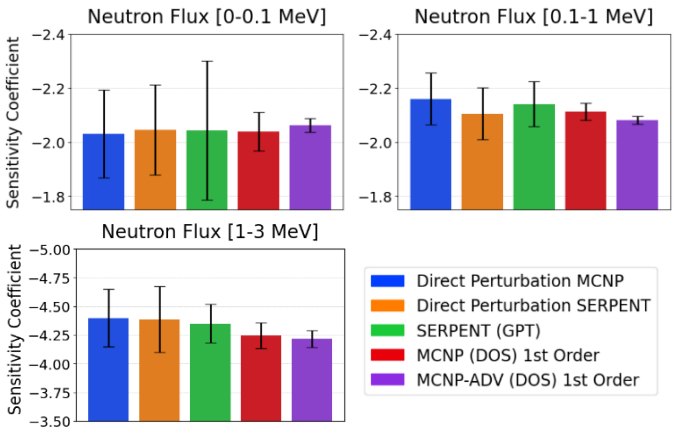

Fig. 3. Sensitivity coefficients for 56Fe integral total cross section with 5% perturbations.

A main concern when using sensitivity coefficients is knowing the maximum magnitude of perturbation that still preserves linear behavior. Beyond this range, a first-order approach can yield inaccurate results, and random sampling methods could be considered instead. The MCNP PERT card allow to obtain perturbed responses for both first and second order perturbations. Figures 4 and 5 show the model's response to perturbations to 56Fe total cross section, with

uncertainties shown as three standard deviations. The ratio displayed includes uncertainties from both the direct perturbation and the PERT cards.

For this system, it is shown that for up to 5% perturbations in the total cross section of 56Fe, the linear approximation remains consistent with direct perturbations. However, beyond this point, the behavior diverges, particularly at higher neutron energies.

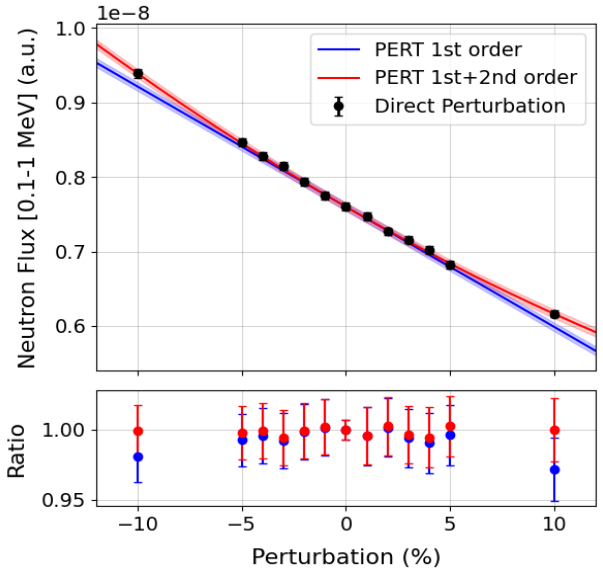

Fig. 4. Comparison of perturbed neutron flux for the 0.1-1 MeV energy range using different order perturbations to 56Fe total cross section

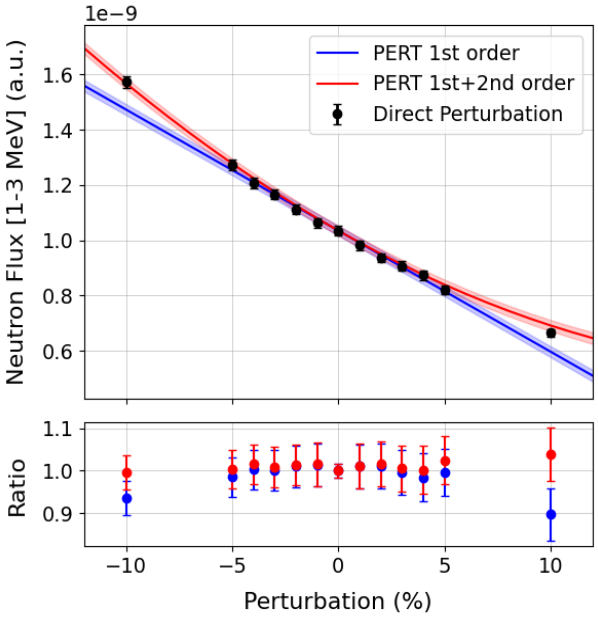

Fig. 5. Comparison of perturbed neutron flux for the 1-3 MeV energy range using different order perturbations to 56Fe total cross section.

Uncertainty Quantification

For uncertainty propagation we considered two major approximations. First, we assumed linearity even though the SCALE covariance matrix includes uncertainties greater than 5% for some cases. This assumption allows us to consider all contributions simultaneously. Second, since the matrix only provides data for total inelastic reactions (MT=4) and not for MT=51 or MT=52, we approximated total inelastic scattering by summing the sensitivities for MT=51 and MT=52.

The propagation of uncertainties was performed using Equation (1), which combines the SCALE matrix and the sensitivity coefficients obtained from the 1st order perturbation PERT sensitivity calculations. This was done using Python-based tool CALINS (CALculation and Investigation on Nuclear data uncertainties and Sensitivities) developed at IRSN. This approach allows us to quantify the impact of nuclear data uncertainties on our calculations.

Table III. Nuclear data uncertainty for neutron flux by energy ranges

Detector Energy (MeV)	Flux per neutron-source	Propagated uncertainty (%)
0-0.1	2.64e-09	5.14
0.1-1	7.65e-09	6.51
1-3	1.07e-09	11.64

Table IV. Major contributors to the propagated variance in neutron flux between 0.1-1 MeV, with the relative contributions of various isotope-reaction pairs.

Nuclide	Reaction	Integral Sensitivity	Relative contribution to the variance (%)
56Fe	ELASTIC	-1.28e+00	49.74
1H	ELASTIC	-3.00e+00	33.15
56Fe	INELASTIC	-7.89e-01	10.47
16O	ELASTIC	-6.91e-01	4.49
54Fe	ELASTIC	-1.47e-01	1.18

Table V. Major contributors to the propagated variance in neutron flux between 1-3 MeV, with the relative contributions of various isotope-reaction pairs.

Nuclide	Reaction	Integral Sensitivity	Relative contribution to the variance (%)
56Fe	ELASTIC	-1.97e+00	55.14
56Fe	INELASTIC	-2.18e+00	27.70
1H	ELASTIC	-2.78e+00	13.83
54Fe	ELASTIC	-2.16e-01	1.82
16O	ELASTIC	-6.13e-01	1.11

Table III shows the values for propagated uncertainties in each energy bin highlighting that these uncertainties approximately double in the energy range of 1-3 MeV, showing the same tendency as the 56Fe sensitivity

coefficients shown in Figure 3. The decomposition of contributors to the variance is examined in Tables IV and V for detector energy ranges of 0.1-1 MeV and 1-3 MeV, respectively. This analysis shows that the same major reaction-isotope pairs contribute to uncertainties in both energy ranges, with iron nuclides having a more significant impact at higher energies. Although hydrogen has the largest sensitivities, it is not the primary contributor to overall uncertainty due to the lower uncertainties associated with its nuclear data. These results demonstrate the feasibility of the approach and provide insights that may show similar trends in PWRs.

The presented uncertainties are calculated by considering correlations between cross sections at different energies and between different reactions for the same isotope, when the data exist. For example, for 56Fe inelastic scattering, contribution to relative variance of neutron flux in the 0.1-1 MeV energy range changes from 0.00755 when only intra-reaction correlations (between energy groups) are considered to 0.00444 when inter-reaction correlations are also included, which is a difference of more than 40%. However, the SCALE 6.1 44-group set provides only partial data on these correlations. Currently, cross-correlations – correlations between reactions of different isotopes – are not considered. Other nuclear data covariances should be analyzed in the future to verify the robustness of the data.

CONCLUSION

This work presents a comparison of sensitivity coefficient calculations for fixed-source problems using different methods in probabilistic codes: GPT in SERPENT and DOS in MCNP. Both methods can provide congruent sensitivity coefficients, but the DOS method allows for the calculation of first plus second-order perturbed responses, enabling an assessment of the applicability of the first-order approach.

Our results, based on the analysis of the 56Fe total cross section, show that for small perturbations (less than 5%), linear approximations can adequately represent the system's behavior, as the error fall within statistical uncertainty. However, to confirm that perturbations are within the linear range, one must verify that the nuclear data uncertainties also fall within this range. This may not always be the case for certain isotopes, such as 56Fe, which often have significant uncertainties associated with their nuclear data. For these cases, sampling method can be a better option.

The use of variance reduction parameters generated by ADVANTG introduced a significant bias in the sensitivity calculations. The authors are currently investigating possible causes for this issue. Some possible sources, including MCNP implicit capture and weight cutoffs, were tested and found not to be contributing factors. In contrast, applying weight windows directly to the geometry cells of the problem yielded better results without introducing bias.

The propagation of uncertainties using the SCALE 6.1 44-group set showed that uncertainties from nuclear data libraries increase at higher neutron flux energies, with iron isotopes contributing the most, followed by water nuclides.

Future work will investigate how this bias observed on the sensitivity coefficients in MCNP affects the results in a cylindrical geometry, such as a PWR vessel, to assess whether ADVANTG can be effectively used in this context. Additionally, we will compare propagated uncertainties obtained through perturbation methods with the ones derived from TMC by perturbing the ACE files, providing a broader comparison for different reactions. We will also explore the use of other covariance matrices with different nuclear data libraries to evaluate the consistency of uncertainty propagation across various datasets.

ENDNOTES

[a]The complete simulation inputs can be accessed at https://gitlab.extra.irsn.fr/jmonleon/vessel-ageing.

REFERENCES

1. D. ROCHMAN et al., “Nuclear Data Uncertainty Propagation: Perturbation vs. Monte Carlo,” Ann. Nucl. Energy, 38, 942-952 (2011).
2. D. G. CACUCI, Handbook of Nuclear Engineering, Vols. 1–4, Springer, (2010).
3. A. GANDINI, “Generalized Perturbation Theory (GPT) Methods: A Heuristic Approach,” in Advances in Nuclear Science and Technology, Springer US, Boston, MA (1987).
4. J. FAVORITE, “Using the MCNP Taylor Series Perturbation Feature (Efficiently) for Shielding Problems,” EPJ Web Conf., 153, 06030 (2017).
5. A. LAUREAU et al., “Uncertainty Propagation Based on Correlated Sampling for Nuclear Data Applications,” EPJ Nucl. Sci. Technol., 6, 8 (2020).
6. M. AUFIERO et al., “A Collision History-Based Approach to Sensitivity/Perturbation Calculations in the Continuous Energy Monte Carlo Code SERPENT,” Ann. Nucl. Energy, 85, 245-258 (2015).
7. V. VALTAVIRTA et al., “Collision-History Based Sensitivity Calculation in Serpent 2.1.30,” BEPU, (2018).
8. P. GRIVEAUX et al., “Computation of Sensitivity Coefficients in Fixed Source Simulations with SERPENT2,” Fusion Eng. Des., 200, 114191 (2024).
9. J. R. LAMPROE et al., “Preliminary Verification of the MCNP Perturbation and Fixed-Source Tally Sensitivity Tools,” Ann. Nucl. Energy, 194, 110040 (2023).
10. ORNL, “SCALE 6.3.1 User Manual — SCALE 6.3.1 [Online]. Available: https://scale-manual.ornl.gov/.
11. S. W. MOSHER et al., “ADVANTG An Automated Variance Reduction Parameter Generator,” ORNL/TM-2013/416, 1105937, (2013).